THE JOURNAL OF PHYSICAL CHEMISTRY Letters

Letter

pubs.acs.org/JPCL

Terms of Use

In Situ, Real-Time Visualization of Electrochemistry Using Magnetic Resonance Imaging

Melanie M. Britton,*[,†] Paul M. Bayley,[‡] Patrick C. Howlett,[‡] Alison J. Davenport,[§] and Maria Forsyth*[,‡]

[†]School of Chemistry, University of Birmingham, Birmingham, B15 2TT, United Kingdom

[‡]Institute for Frontier Materials, Deakin University, Burwood, Victoria, 3125 Australia

[§]School of Metallurgy and Materials, University of Birmingham, Birmingham, B15 2TT, United Kingdom

Supporting Information

ABSTRACT: The drive to develop better electrochemical energy storage devices requires the development of not only new materials, but also better understanding of the underpinning chemical and dynamical processes within such devices during operation, for which new analytical techniques are required. Currently, there are few techniques that can probe local composition and transport in the electrolyte during battery operation. In this paper, we report a novel application of magnetic resonance imaging (MRI) for probing electrochemical processes in a model electrochemical cell. Using MRI, the transport and zinc and oxygen electrochemistry in an alkaline electrolyte, typical of that found in zinc-air batteries, are investigated. Magnetic resonance relaxation maps of the electrolyte are used to visualize the chemical composition and electrochemical processes occurring during discharge in this model metal-air battery. Such experiments will be useful in the development of new energy storage/conversion devices, as well as other electrochemical technologies.

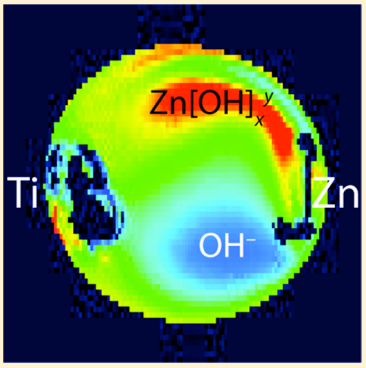

SECTION: Energy Conversion and Storage; Energy and Charge Transport

Magnetic resonance imaging (MRI) has long been recognized as a leading technique in medical diagnosis and biomedical research. However, what makes this technique an excellent tool for imaging the brain, for example, also makes it highly effective for noninvasively studying complex, spatially heterogeneous chemical systems.[1] In this context, MRI has already made important contributions in the fields of materials, reaction engineering and catalysis. There have, however, been considerably less applications of MRI for electrochemical systems. This is largely due to the experimental challenges associated with the imaging artifacts caused by the metals commonly found in electrochemical cells.[2−7] While, there are a number of papers in the literature investigating the origins and minimization of MRI artifacts associated with the presence of metal, particularly in medical research, these have not demonstrated that signal distortions can be eliminated sufficiently near a metal surface and that viable information about electrochemical processes can be obtained in these regions, where critical changes in the electrolyte chemistry are expected for many of the underpinning electrochemical processes found in batteries, fuel cells, corrosion and metal electrofinishing.

In this paper, we demonstrate how the challenges of imaging near metal surfaces can be overcome and demonstrate how in situ electrochemical MRI has enormous potential for better understanding and development of energy devices such as batteries and fuel cells, and can also be extended to investigate electrochemical processes in corrosion and metal electrofinishing. In such applications, there are currently very few techniques that are able to probe local behavior in the electrolyte leading to in situ characterization of metal/electrolyte interactions, particularly near the interface, which is the focus of this study. Thus in this paper, we will demonstrate new advanced analytical methods to study the chemical and dynamical processes of electrochemical systems in situ, in real-time and spatially resolved. This addresses one of the primary challenges in understanding and thereby advancing many electrochemical technologies including energy storage, metal finishing and corrosion prevention.

The use of MRI to study electrochemical systems has only seen limited interest from the research community to date.[8−10] Grey et al.[8] have recently shown that in situ NMR characterization of a lithium battery in different electrolytes provides unique insights into the interfacial chemistry, in particular the onset of dendritic metal deposition, occurring at the lithium anode. We have also shown[9] that MRI can be used to visualize corrosion of zinc wire in a highly concentrated chloride ion solution. Here we report, for the first time, visualization of a complete zinc cell in a high pH solution typically found in a zinc−air battery. We investigate the cell during discharge for more than 48 h and follow the effect of polarization of the cell over time. Furthermore, we observe the unexpected behavior of zinc corrosion upon application of

Received: July 9, 2013
Accepted: August 22, 2013
Published: August 22, 2013

 © 2013 American Chemical Society

imaging gradients in this electrolyte, even at open circuit (in the absence of load). This is most likely an effect of potential differences in the metal being established due to eddy currents that arise[2] when the imaging gradients are switched on.

It is well-known that MRI is problematic in systems containing metals and has been well documented in medical imaging[2−7] where image artifacts occur when patients have nonferromagnetic metal implants in their body, such as stents or dental castings. These artifacts occur for several reasons, notably susceptibility differences with surrounding material causing additional magnetic field gradients,[2] eddy currents due to RF or magnetic field gradient switching[4] and RF inhomogeneity.[11] For the same reasons, MRI measurements of electrochemical processes where a metallic component is present, such as the zinc anode in a Zn-air battery, is not a trivial matter. However, we have found that optimization of the orientation of the zinc electrode with respect to the radio frequency (r.f.) (B_1) field minimizes distortions and allows measurement of undistorted voxels close to the metal surface, as illustrated in Figure 1. It was found that the shape and

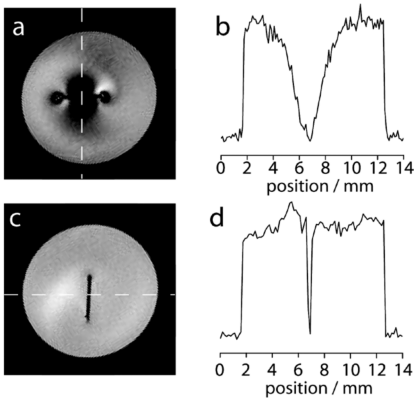

Figure 1. Proton spin-density MR images showing the orientation dependence of zinc metal in 1 M NaOH solution. In the images, the metal strip is normal (a) and parallel (c) to the radiofrequency (B_1) field. The profiles in (b) and (d) are taken normal to the metal strips in (a) and (c), respectively. Images have a field of view of 14 × 14 mm^2 and a slice thickness of 2 mm.

orientation of the metal strongly influenced the image. By using metal strips, rather than wires, and by aligning them vertically in the static magnetic field (B_0) and parallel to the B_1 field, the imaging artifacts could be mostly eliminated. We believe the artifacts due to a variation in the strength of the r.f. field,[11] which locally modulates the signal around the metal, causing image distortions.

By adopting these geometry constraints, it is possible to construct a cell, which can be imaged using MRI, by aligning the metal electrodes with respect to the B_1 field. A schematic of the electrochemical cell developed for this work is shown in Figure 2, which comprises Zn with Ti, to support the cathode reaction in this simplified cell arrangement, in an electrolyte of 1 M NaOH solution. MRI data obtained for the electrochemical cell containing both Zn and Ti metal strips at open circuit shows the immediate appearance of distinct features in the magnetic resonance (MR) T_1 relaxation times of the water in the electrolyte (Figure 3a). This variation in T_1 suggests compositional changes in the electrolyte, most likely to be dominated by changes in the concentration of hydroxide ions in the electrolyte (Figure 3b). Curiously, these variations in T_1 are

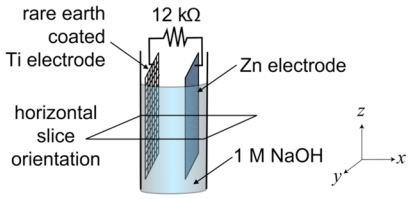

Figure 2. Schematic representation of the full Zn−air cell when under the constant load discharge condition, illustrating the horizontal image orientation. The diameter of the vial is 12 mm.

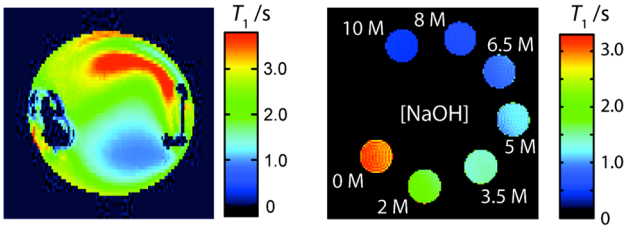

Figure 3. Horizontal ^{1}H MR T_1 maps for (a) a cell containing 1 M NaOH solution and unconnected Ti (left) and Zn (right) strips and (b) a phantom sample comprising seven 5 mm NMR tubes containing NaOH solutions at a range of concentrations (0−10 M). T_1 maps were created from seven spin−echo images with inversion recovery delays of 30−1500 ms, and a 25 × 25 mm^2 field of view and 2 mm slice thickness.

also observed for NaOH solution in the presence of Zn metal only (Figure 4). In the vertical images shown in Figure 4, it can been seen that there is a correlation between the MR T_1 and T_2 relaxation measurements and that the compositional changes observed in the relaxation maps are also associated with motion in the electrolyte, as observed by velocity measurements (Figure 4c). The velocity pattern is typical of a convection current, and it seems there is a relationship between the induced motion and the compositional changes detected in the relaxation maps. Convection has been previously observed in anodic zinc dissolution in hydroxide solutions[12] in a magnetic field, where convection was caused by the Lorentz force acting on the ions in solution.[13]

The observation of these features, when zinc was imaged in the NaOH electrolyte, both in the presence and absence of the titanium, was unexpected. Such behavior was not observed when other electrolyte solutions, including concentrated LiCl and pure water, were investigated (as shown in the images in the Supporting Information (Figure S1)). Therefore, it suggests the relaxation maps obtained represent chemical changes in the electrolyte resulting from electrochemical processes between the NaOH electrolyte and zinc. How these occur in an isolated strip of zinc metal, therefore, needs to be rationalized.

It is well-known that the magnetic field gradient switching can generate eddy currents in conducting materials.[14] Furthermore, the strong B_0 field causes asymmetric charge distribution across the zinc metal, according to the Hall effect, that will contribute to establishing a difference in potential across the length of the zinc strip. Such a potential difference, in an appropriate environment, can establish an electrochemical reaction (or corrosion cell). The electrochemical processes occurring at the Zn metal/electrolyte interface under such conditions involve oxygen reduction on one side of the zinc, generating four hydroxide ions, while Zn^{2+} ions are being produced at the anodic site. Importantly, this model is

dx.doi.org/10.1021/jz401415a | J. Phys. Chem. Lett. 2013, 4, 3019−3023

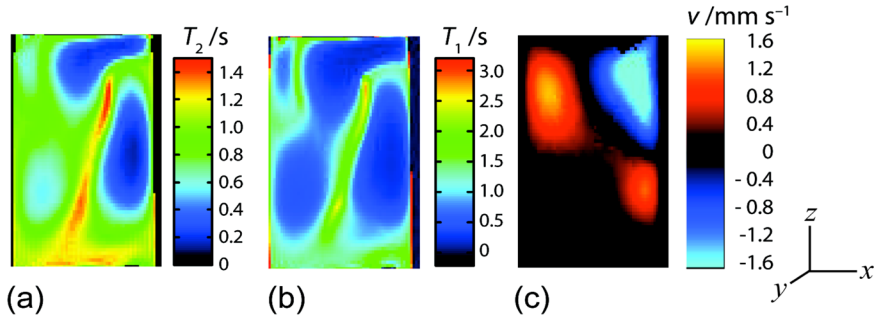

Figure 4. Vertical maps of (a) T_2 and (b) T_1 MR relaxation times and (c) velocity (v_z) for a cell containing a Zn strip only in 1 M NaOH solution. In all images, the Zn strip is on the right side of the cell. A region of 19 (z) × 12 (x) mm^2 is shown in each image.

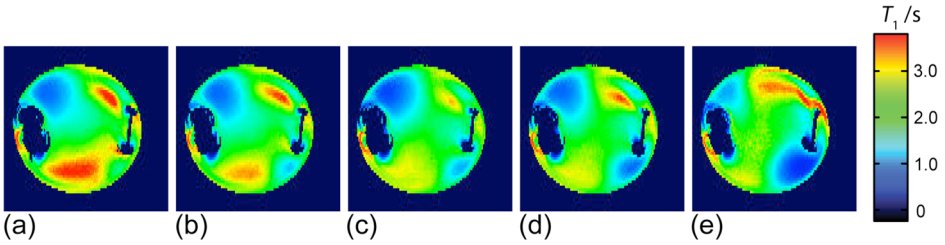

Figure 5. Horizontal ^{1}H MRI T_1 maps of the full Zn−air cell under constant load discharge at 12 kΩ. Experiment conducted close to complete cell failure. Images were acquired upon connection (a), 11 h (b), 23 h (c), 30 h (d) and 47 h (e). The Zn strip is on the right. MRI parameters are the same as in Figure 3.

supported by our observation that large pits were formed on some of the zinc metal specimens exposed to imaging gradients, even after short imaging times, a phenomenon not reproduced in any of the control experiments, where electrolytes other than hydroxide were used (Figure S1), or where the cell was observed outside the magnet. In these control measurements, corrosion over the same time-scale was not observed.

The shape of the features on the horizontal T_1 map (Figure 3a) are therefore interpreted as follows: zincate ions ($[Zn(OH)_4]^{2-}$) form under anodic potentials and stream into the solution leading to a lower concentration of OH^- (observed as an increase in T_1 (red) at the top of the image). These large, highly associated negatively charged ions appear to be transported from the top of the Zn electrode under the influence of convection. Hydroxide ions are produced by the oxygen reduction reaction at the more cathodic potentials, forming the lower T_1 (blue) region observed at the bottom of the image. Velocity imaging of the electrolyte (Figure 4c) supports the presence of convection. However, convection alone cannot produce the T_1 variations observed in the T_1 maps of this system. Hence convection must be coupled with compositional changes, such as the variation in concentration of zincate and hydroxide ions that are formed due to the electrochemical reactions, which in the case of the open circuit cells are induced by the imaging gradients.

The effect of connecting the Ti and Zn electrodes, thus forming a zinc−oxygen cell, was also investigated. Once connected, imaging was performed throughout constant load discharge over several hours. Figure 5 shows the T_1 relaxation maps throughout this process. Initially the cell appears to be operating as intended, based on our interpretation, with the longest T_1 features representing the transport of zincate ions away from the zinc anode, and very short T_1 features from hydroxide ions being produced on the titanium cathode (see Figure 6). This condition however, quickly reverts and images resembling those of the cell at open circuit are observed, with

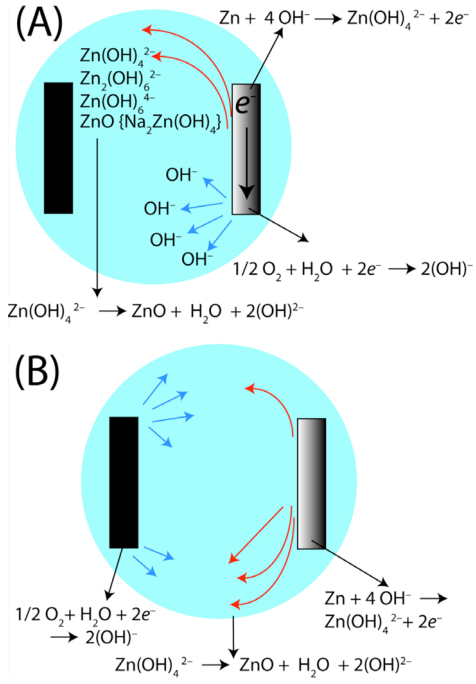

Figure 6. Schematic representation of the interpretation of the horizontal images at open-circuit (A) and during the initial stages of constant load discharge (B). The rare-earth coated titanium mesh electrode is depicted on the left of each cell with the zinc on the right.

the hydroxide feature growing on the zinc and receding at the titanium. As the cell is discharging and there is a build up of ZnO (and a small amount of sodium zincate that will consume tiny amounts of water) on the Zn electrode surface, the cell consequently becomes polarized such that it can no longer sustain substantial discharge currents as intended. At this point we essentially have open circuit conditions, with negligible net

dx.doi.org/10.1021/jz401415a | J. Phys. Chem. Lett. 2013, 4, 3019−3023

electrode reactions occurring. Thus the electrochemical processes revert back to those shown in Figure 6a, where both the anodic and cathodic reactions will occur on the zinc metal due to potential differences imposed by the eddy currents in the metal. At 23 h into discharge (Figure 4), the reaction appears to be in mid-transition between these two extremes. As the resistivity of the metal/electrolyte surface increases and the cell continues to polarize, the production of zincate ions is expected to diminish, as visualized by a large reduction in the zincate (low T_1) feature.

If we consider now the magnitude of the T_1 values shown (Figures 3−5), we can correlate these with our electrochemical explanations (Figure 6). The regions where we hypothesize zincate ions form have a significantly larger T_1 than bulk (red) and the region where oxygen reduction reaction produces more OH^- has a lower T_1 than bulk (blue). Thus, qualitatively, the cathodic reaction leads to a lowering of T_1 as the OH^- ions are produced while the anodic reaction, where the zincate complexes are generated at the metal/electrolyte interface, leads to an overall reduction in OH^- concentration and thus an increase in T_1. T_1 values measured as a function of [NaOH], using an inversion recovery pulse sequence, are shown in Figure S2. Spatial variation in the observed T_1 values, compared with bulk T_1 most likely arise purely from composition;[1] however, it is possible that an electric field may also influence T_1, where effects have previously been reported,[15] albeit for extreme voltages of the order of 1000 V/mm in molecular solvents. This needs further investigation, particularly for the concentrated electrolyte systems typically found in electrochemical devices.

This work shows that useful information describing the compositional and physical environment in an electrochemical cell can be obtained using in situ MRI methods, which could ultimately lead to improved characterization of the performance of metal air cells. Importantly, a greater understanding of the influence of a strong magnetic field on the performance of electrochemical devices will improve our interpretation of these measurements and how they relate to the real application environment. In combination with the recently demonstrated[8] method of in situ imaging a lithium electrode, we have shown that it is possible to simultaneously gather detailed information on both the electrode and electrolyte, an encouraging prospect. However, with polarization of the cell at longer times leading to electrochemistry induced by the imaging gradients and not necessarily due to the cell discharge, care must be taken to ensure the applicable electrochemical conditions of the system of interest are maintained in the device. Thus, only the early stages of cell discharge could be reliably imaged in this initial work. However, we are confident that these issues can be resolved by adapting the cell, imaging parameters and/or suppressing convection, as well as controlling the current/potential using a potentiostat. This application of MRI opens exciting opportunities to develop a greater theoretical and practical understanding of the origin of the observed effects and to further develop a unique tool for imaging electrochemical processes that occur in technologically important applications such as energy storage and corrosion assessment.

We have demonstrated that careful design and construction of an electrochemical cell enables the composition and molecular mobility within the electrolyte to be imaged, in situ and in real-time. We have found that for Zn in NaOH solution, the imaging gradients are able to affect electrochemical processes in the system, though, the presence of the Hall effect and the origins of convection require further investigation and verification. However, we have shown that this effect is not observed in all systems, and as we are able to produce unique in situ measurements of electrochemical processes in an operating cell, not accessible with other methods, we feel that this methodology is worthy of investigating further to determine how these effects can be minimized or eliminated.

■ ASSOCIATED CONTENT

Ⓢ Supporting Information

Experimental details, T_1 relaxation plots versus [NaOH], and control sample MR images are provided in the Supporting Information. This material is available free of charge via the Internet at http://pubs.acs.org.

■ AUTHOR INFORMATION

Corresponding Authors

*E-mail: m.m.britton@bham.ac.uk.
*E-mail: maria.forsyth@deakin.edu.au.

Notes

The authors declare no competing financial interest.

■ ACKNOWLEDGMENTS

The authors acknowledge funding from the Australian Research Council through grants LE110100141 (supporting the NMR facility) and FL110100013 (Australian Laureate fellowship) and through the ARC Centre of Excellence for Electromaterials Science (ACES). The authors are also grateful to the EPSRC UK granting scheme for funding the initial collaboration through an EPSRC Visiting Professorship Grant.

■ REFERENCES

(1) Britton, M. M. Magnetic Resonance Imaging of Chemistry. *Chem. Soc. Rev.* **2010**, *39*, 4036−4043.
(2) Bennett, L. H.; Wang, P. S.; Donahue, M. J. Artifacts in Magnetic Resonance Imaging from Metals. *J. App. Phys.* **1996**, *79*, 4712−4714.
(3) Camacho, C. R.; Plewes, D. B.; Henkelman, R. M. Non-susceptibility Artifacts Due to Metallic Objects in MR-Imaging. *J. Magn. Reson. Imaging* **1995**, *5*, 75−88.
(4) Graf, H.; Steidle, G.; Martirosian, P.; Lauer, U. A.; Schick, F. Effects on MRI due to Altered RF Polarization Near Conductive Implants or Instruments. *Med. Phys.* **2006**, *33*, 124−127.
(5) Olsen, R. V.; Munk, P. L.; Lee, M. J.; Janzen, D. L.; MacKay, A. L.; Xiang, Q. S.; Masri, B. Metal Artifact Reduction Sequence: Early Clinical Applications. *Radiographics* **2000**, *20*, 699−712.
(6) Shafiei, F.; Honda, E.; Takahashi, H.; Sasaki, T. Artifacts from Dental Casting Alloys in Magnetic Resonance Imaging. *J. Dent. Res.* **2003**, *82*, 602−606.
(7) Viano, A. M.; Gronemeyer, S. A.; Haliloglu, M.; Hoffer, F. A. Improved MR Imaging for Patients with Metallic Implants. *Magn. Reson. Imag.* **2000**, *18*, 287−295.
(8) Chandrashekar, S.; Trease, N. M.; Chang, H. J.; Du, L. S.; Grey, C. P.; Jerschow, A. Li-7 MRI of Li Batteries Reveals Location of Microstructural Lithium. *Nat. Mater.* **2012**, *11*, 311−315.
(9) Davenport, A. J.; Forsyth, M.; Britton, M. M. Visualisation of Chemical Processes during Corrosion of Zinc using Magnetic Resonance Imaging. *Electrochem. Commun.* **2010**, *12*, 44−47.
(10) Klett, M.; Giesecke, M.; Nyman, A.; Hallberg, F.; Lindstrom, R. W.; Lindbergh, G.; Furo, I. Quantifying Mass Transport during Polarization in a Li Ion Battery Electrolyte by in Situ Li-7 NMR Imaging. *J. Am. Chem. Soc.* **2012**, *134*, 14654−14657.
(11) Vashaee, S.; Newling, B.; MacMillan, B.; Balcom, B. J. B_1 Mapping with a Pure Phase Encode Approach: Quantitative Density Profiling. *J. Magn. Reson.* **2013**, *232*, 68−75.

(12) Mogi, I.; Kikuya, H.; Watanabe, K.; Awaji, S.; Motokawa, M. Magnetic Field Effects on the Current Oscillations in Anodic Zinc Dissolution. *Chem. Lett.* **1996**, 673−674.
(13) Nishikiori, R.; Morimoto, S.; Fujiwara, Y.; Tanimoto, Y. Magnetic Field Effect on the Cathodic Potential Oscillation of Zinc Electrode in Alkaline Solution. *Appl. Magn. Reson.* **2011**, *41*, 221−227.
(14) Han, H.; Green, D.; Ouellette, M.; MacGregor, R.; Balcom, B. J. Non-Cartesian Sampled Centric Scan SPRITE Imaging with Magnetic Field Gradient and $B_0(t)$ Field Measurements for MRI in the Vicinity of Metal Structures. *J. Magn. Reson.* **2011**, *206*, 97−104.
(15) Jones, G. P.; Bradbury, A.; Bradley, P. A. Electric-Field Induced Changes of Spin-Lattice Relaxation-Time T_1 in Polar Liquids. *Mol. Cryst. Liq. Cryst.* **1979**, *55*, 143−149.